

RSC Advances



This is an *Accepted Manuscript*, which has been through the Royal Society of Chemistry peer review process and has been accepted for publication.

Accepted Manuscripts are published online shortly after acceptance, before technical editing, formatting and proof reading. Using this free service, authors can make their results available to the community, in citable form, before we publish the edited article. This *Accepted Manuscript* will be replaced by the edited, formatted and paginated article as soon as this is available.

You can find more information about *Accepted Manuscripts* in the [Information for Authors](#).

Please note that technical editing may introduce minor changes to the text and/or graphics, which may alter content. The journal's standard [Terms & Conditions](#) and the [Ethical guidelines](#) still apply. In no event shall the Royal Society of Chemistry be held responsible for any errors or omissions in this *Accepted Manuscript* or any consequences arising from the use of any information it contains.

Research Highlights

- 1) Two new fluorescent PET chemosensors were designed and synthesised from acridine core.
- 2) Sensors can be used to monitor Cu^{2+} and Al^{3+} in CH_3CN .
- 3) The detection limits for **7a**- Cu^{2+} and **7b**- Al^{3+} were calculated to be 2.8×10^{-7} M and 5.8×10^{-7} M, respectively.
- 4) Binding study of metals to the probes showed that the nature of receptor plays very important role in the selective detection of metal ions.

A highly sensitive and selective chemosensors for Cu²⁺ and Al³⁺ based on photoinduced electron transfer (PET) mechanism

Santosh Chemate, Nagaiyan Sekar*

Tinctorial Chemistry Group, Department of Dyestuff Technology, Institute of Chemical Technology, Mumbai- 400 019 (India)

Email: n.sekar@ictmumbai.edu.in, nethi.sekar@gmail.com Tel: + 91 22 3361 2707.

Abstract: Two novel acridine based chemosensors **7a** and **7b** were synthesized and configured as “fluorophore-spacer-receptor” systems based on photoinduced electron transfer. The probes **7a** and **7b** exhibited high selectivity and sensitivity for the detection of Cu²⁺ and Al³⁺ respectively over commonly coexistent metal ions in CH₃CN. The binding association constants (*K_a*) of **7a**-Cu²⁺ and **7b**-Al³⁺ were obtained to be 4.0 x 10⁴ M⁻¹ and 1.7 x 10⁴ M⁻¹ in CH₃CN, and the corresponding detection limits were calculated to be 2.8 x 10⁻⁷ M and 5.8 x 10⁻⁷ M, respectively. The fluorescence response of **7a**-Cu²⁺ and **7b**-Al³⁺ with respect to pH change was studied and the result demonstrated fluorescence enhancement was observed in the pH range of 7.0 - 9.0. The chromophores were characterized by FT-IR, ¹H-NMR, ¹³C-NMR and HR Mass spectral analysis.

Keywords: Metal sensors, acridine, emission, copper, aluminum, quantum yield.

1. Introduction

The designing and synthesis of fluorescent chemosensors for transition metal ions in various biological systems are of growing interest because of their fundamental role in chemical and biological processes¹⁻⁶. Copper is the third most abundant transition metal ion (after Fe²⁺ and Zn²⁺) in human body and is involved in various metabolic processes such as copper combines with proteins to produce enzymes involved in oxygen processing and also acts as a catalyst in body functions⁷⁻⁹. It is an essential element at very low concentration for all the organisms but in high concentration it is

hazardous to living organisms. Wherever excess concentration of Cu^{2+} in human body causes severe neurological diseases such as Alzheimer's disease, Menkes, Wilson's disease and Parkinson's disease¹⁰⁻¹². Recently copper ions in prolonged exposure to human body have been suspected to cause children's liver and kidneys damage¹². Therefore it is important to detect copper at very low concentration in the biological systems. It is also observed that Cu^{2+} deficiency leads to severe fatal problems in animals^{13,14} thus the deficiency or excessive intake of Cu^{2+} is very harmful and this demands development of molecular probe for selective detection of Cu^{2+} ion.

Aluminum plays very imperative role in human life and happens to be the third most abundant element and the most abundant metal in the earth's crust (approx. 8% by mass). Because of high chemical reactivity of aluminum metal it gets easily converted to Al^{3+} due to acid rain and human activities^{15,16}. Aluminum compounds are also frequently utilized as pharmaceutical drugs in human and veterinary medicine^{17,18}. Among them, buffered aspirin containing aluminum glycinate is commonly used as an analgesic¹⁹ as well as in antacid^{20,21}. Accumulation of excessive amounts of Aluminum metal damages the kidney^{22,23}, central nervous system causing Alzheimer's disease^{24,25}, it reduces total bone and matrix causing osteoporosis, osteomalacia^{26,27} and kills fish in acidic water²⁸. The incremental increase of Al^{3+} concentrations in the environment disturbs the growing plants^{29,30}. Recently C. Exley and co-workers reported that excess intake of aluminum-based antiperspirants causes breast cancer in woman¹⁷. Thus the development of fluorescent chemosensor for detection of hazardous metal ion is having more importance for biological and environmental aspect.

Several methods are in practice for the detection of metal ions like atomic absorption spectrometry³¹, liquid-phase chromatography³², solid-phase extraction³³, X-ray fluorescence³⁴, inductively coupled plasma mass spectrometry³⁵ and voltammetry³⁶. Most of these techniques are expensive, time consuming as well less susceptible for biological systems and in environmental

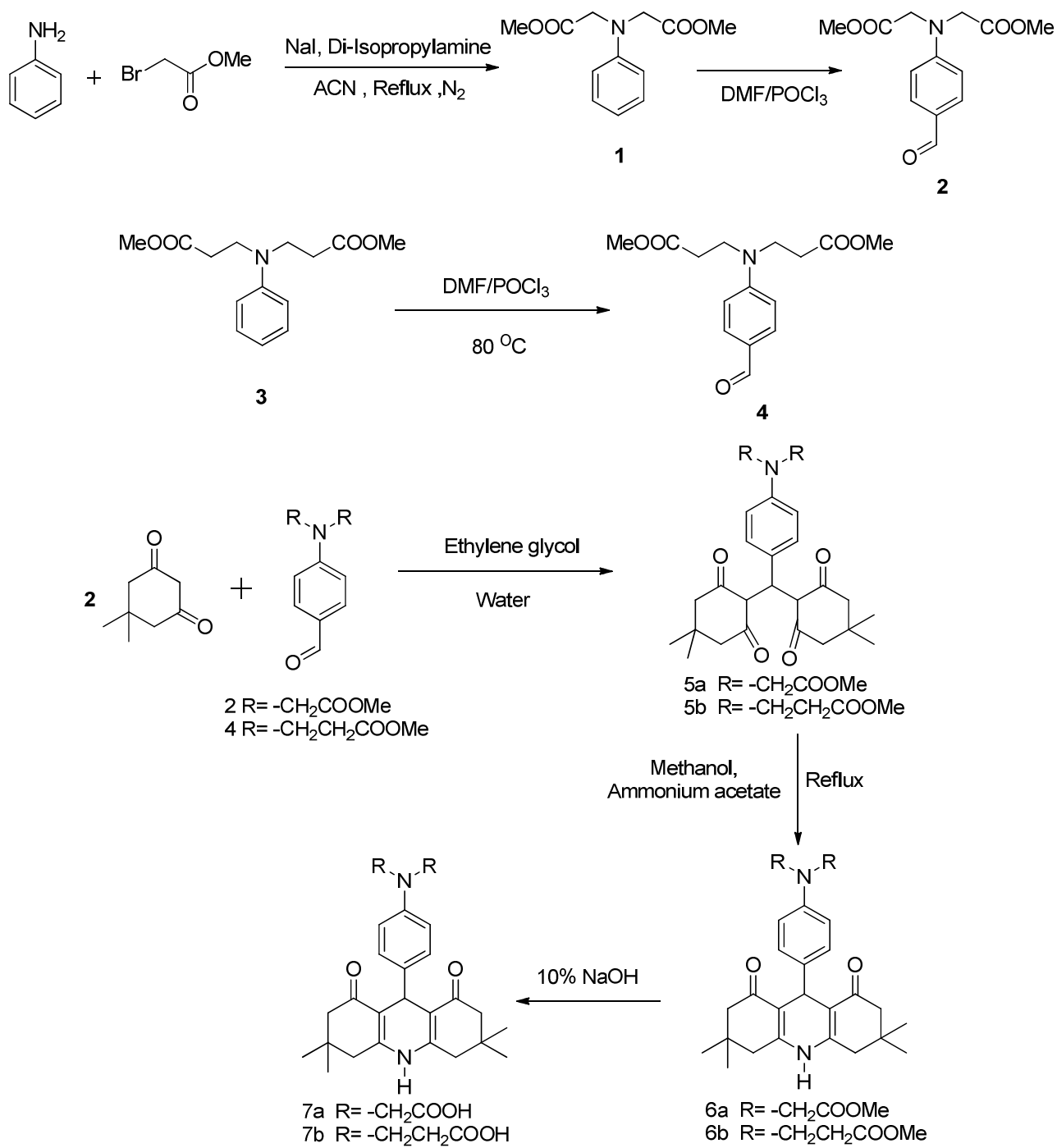
media. This demands for the development of chemosensor that can work for all samples in physiological conditions³⁷.

A variety of fluorescent chemosensor for Cu^{2+} are reported based on fluorescence resonance energy transfer (FRET)³⁸, intramolecular charge transfer (ICT)³⁹, photoinduced electron transfer (PET)⁴⁰, excimers based⁴¹ and chelation enhanced fluorescence (CHEF)⁴². Compared to the transition metals, the detection of Al^{3+} has always been challenging and problematic due to the poor coordination ability⁴³ but few sensors for Al^{3+} are reported⁴⁴⁻⁴⁹. However, there is still scope for improvement in the design of such sensors as they often suffer some problems such as narrow pH range, less selectivity, less response time, unfavourable absorption emission, stability, synthesis cost and low fluorescence quantum yield. From the available sensor most of the fluorescent sensors are based on the PET mechanism, in which enhancement or quenching in fluorescence intensity is observed. A typical fluorescent sensor contains a receptor (the recognition site) linked to a fluorophore (the signal source) which translates the recognition event into the fluorescence signal⁵⁰. Thus the receptor unit must have strong binding affinity to the relevant target. Photoinduced electron transfer based sensor (PET) usually have three components such as *fluorophore-spacer-receptor* in which the ionic or molecular input at receptor site modulate the emission such as fluorescence quantum yield, lifetime and leads to On-Off or Off-On sensing mechanism⁵¹. The choice of the receptor totally depends on the target analytes. In the present paper, we have presented PET based sensors for Cu^{2+} and Al^{3+} in presence of other metal ions in CH_3CN . The binding study of metals to the probe shows that nature of receptor plays very important role in selective detection of metal ions. The studied chromophores shows fluorescence turn on response to Cu^{2+} and Al^{3+} , based on classical photoinduced electron transfer (PET) principle developed by de Silva^{52,53} and are stable for the pH range 7.0-9.0.

2. Results and Discussion

2.1. Chemistry

The acridine derivatives **7a** and **7b** were synthesized by substitution, formylation and addition type of reactions. The intermediate **1** was prepared from aniline and methyl bromoacetate in basic media by nucleophilic substitution reaction which was further converted to the compound **2** by formylation reaction⁵⁴. The intermediate **4** was prepared by formylation of the compound **3** in DMF/POCl₃ at 80 °C. The intermediate **2** and **4** were reacted with dimedone undergoes classical Knoevenagel condensation leads to the formation of the tetraketone **5a-b**, which on cyclization in presence of ammonium acetate in methanol leads to formation of the acridine esters **6a-b**. Hydrolysis of acridine esters in 10% NaOH leads to formation of **7a-b**. The structures of the dyes were confirmed by FT-IR, ¹H NMR, ¹³C NMR and mass spectral analysis. The synthetic details are presented in **Scheme 1**.

Scheme 1: Synthesis of acridine sensors **7a** and **7b**

2.2. Absorption and emission properties

2.2.1. Metal sensing study

The binding activities of the sensors **7a** and **7b** with various metal ions such as Zn^{2+} , Hg^{2+} , Cd^{2+} , Fe^{2+} , Ba^{2+} , Mn^{2+} , Ni^{2+} , Mg^{2+} , Co^{2+} , Cu^{2+} , Cu^+ , Ag^+ , Na^+ , K^+ and Al^{3+} were investigated by UV-visible absorption and fluorescence spectroscopy. The free probes **7a** (20 μM) and **7b** (20 μM) exhibited two absorption peaks at 305 and 365 nm in CH_3CN . With the addition of Cu^{2+} (5 equiv.) to the probe **7a** (20 μM) in CH_3CN , the absorption peak at 305 nm disappeared. In contrast, no significant change was observed for the absorption band at 365 nm (Fig. S1, ESI[†]). The addition of Al^{3+} (5 equiv.) to the probe **7b** (20 μM) leads to decrease in the absorbance at 365 nm while the absorption peak at 305 nm disappeared (Fig. S2, ESI[†]). However, no remarkable change in absorption spectra was observed after addition of other metal ions to probe **7a** and **7b**. Upon the addition of increasing concentration of Cu^{2+} (0 to 5 equiv.) to the probe **7a** (10 μM) slight increase in the absorbance was observed at 365 nm while the absorption peak at 305 nm gradually disappeared (Fig. S3, ESI[†]). A similar trend was observed for the addition of Al^{3+} (0 to 5 equiv.) to **7b** (10 μM) in CH_3CN (Fig. S4, ESI[†]). In addition, the fluorescence spectrum was obtained by excitation at 365 nm. In the absence of metal ions the probes **7a-b** showed very weak fluorescence signal in the range from 420 to 440 nm in CH_3CN . Upon the addition of Cu^{2+} (5 equiv.) to **7a** (20 μM) and Al^{3+} (5 equiv.) to **7b** (10 μM) significant enhancement in the fluorescence intensity was observed at 420-440 nm (Fig. 1 - 2). Whereas no considerable change in the fluorescence intensity was observed for other metal ions.

Please Insert **Fig. 1** and **Fig. 2**

To investigate the interaction of Cu^{2+} with probe **7a** and Al^{3+} with probe **7b**, the emission spectra with varying Cu^{2+} and Al^{3+} concentrations in CH_3CN were recorded separately. Fluorescence intensity of the probe **7a** (10 μM) reaches a maximum when 5 equivalent of Cu^{2+} was added (Fig. 3). After

addition of 5 equivalent of Cu^{2+} to probe **7a** (10 μM), a blue shifted emission from 429 nm to 420 nm (~9 nm) was observed. However, the fluorescence intensity of **7b** (10 μM) increases gradually at 425 nm upon addition of increasing concentration of Al^{3+} (0 to 5 equiv.) in CH_3CN (Fig. 4) while no shift in maximum emission was observed. It is, thus, expected that there is appreciable interaction between the probe **7a** and **7b** with Cu^{2+} and Al^{3+} respectively.

Please Insert **Fig. 3** and **Fig. 4**

From the photophysical properties it is observed that the binding of the sensors **7a-b** to Cu^{2+} and Al^{3+} ion takes place by electrostatic interactions between $-\text{COOH}$ and nitrogen atom present in the receptor part of the molecule (Fig. 5). By conjugating a receptor into the metal ion, the binding would perturb the energy levels of the excited states, which results in a change of emission wavelength. The sensing ability depends on size of receptor, spacer and availability of binding units which forms coordination complex with metal ions. It also depends upon the geometry of the coordination complex formed after ligand to metal binding. The Cu^{2+} and Al^{3+} have different chemical coordination characteristics. Thus, the sensor **7a** is connected to the receptor by a short spacer which shows selective fluorescence enhancement to Cu^{2+} ion while for sensor **7b**, the receptor is connected to fluorophore by long spacer which shows strong selectivity and sensitivity to Al^{3+} ion.

Please Insert **Fig. 5**

The selectivity of the probe **7a** (10 μM) was studied in the presence of other competitive metal ions. The competition experiments revealed that the Cu^{2+} induced fluorescence enhancement was unaffected in 5 equivalent of environmentally relevant alkali or alkaline-earth metals, such as Na^+ , K^+ and Mg^{2+} as well as the other transition metal ions Zn^{2+} , Ni^{2+} , Cd^{2+} , Co^{2+} , Mn^{2+} , Fe^{2+} (Fig. 6). Obviously, all of these results confirmed that our proposed chemosensor **7a** (10 μM) has remarkably high selectivity

toward Cu^{2+} ions over the other competitive metal ions in CH_3CN . The similar observations are observed for the sensor **7b** in presences of other metal ions (Fig. 7).

Please insert **Fig. 6** and **Fig. 7**

The quantum yields of free sensors as well as metal-sensor complex were evaluated by relative method.

The fluorescence quantum yields of **7a** without and with Cu^{2+} were 0.083 and 0.85, respectively. Thus 10 fold increase in fluorescence quantum yield of the sensor **7a** was observed after binding with Cu^{2+} in CH_3CN . In the case of sensor **7b**, 15 fold increase in quantum yield was observed for **7b**- Al^{3+} complex (0.81) as compared to free sensor (0.054). The change in fluorescence intensity of the probe **7a** (10 μM) in 5 eq. of Cu^{2+} in $\text{CH}_3\text{CN}/\text{H}_2\text{O}$ mixture was studied at pH 9.0. Notably, we observed that the fluorescence intensity remains unaltered up to 60% CH_3CN and 40% H_2O mixture. However, further increase in H_2O concentration leads to slight decrease in the fluorescence intensity (Fig. S5, ESI[†]).

The effect of pH on **7a**, **7b** and their complexes **7a**- Cu^{2+} , **7b**- Al^{3+} were studied from pH range 3-12. The fluorescence intensity of the sensors **7a** and **7b** decreases from pH 3 to 7 and after it remains constant till pH = 12. The fluorescence intensity of **7a**- Cu^{2+} complex increases slightly from pH 3 to pH 7 and after that remains constant up to pH 12. In case of **7b**- Al^{3+} complex fluorescence intensity slightly increases from pH 3 to pH 7 and it remains constant from pH 7 to pH 9. After pH 9 the fluorescence intensity of **7b**- Al^{3+} complex decreases suddenly because of hydrolysis of Al^{3+} in basic condition (Fig. S6, ESI[†]). At lower pH both the probes **7a** and **7b** showed high fluorescence intensity. In acidic pH conditions the protonation of aromatic amine nitrogen takes place which suppress photoinduced electron transfer mechanism.

The binding association constant (K_a) for **7a**-Cu²⁺ and **7b**-Al³⁺ were determined from Benesi-Hildebrand equation. The binding association constants of **7a** with Cu²⁺ and **7b** with Al³⁺ were observed to be $4.0 \times 10^4 \text{ M}^{-1}$ and $1.7 \times 10^4 \text{ M}^{-1}$, respectively. The estimated limit of detection (LOD) came out to be $2.8 \times 10^{-7} \text{ M}$ for **7a**-Cu²⁺ and $5.8 \times 10^{-7} \text{ M}$ for **7b**-Al³⁺ complex in CH₃CN (Fig. S7, ESI †) and compared with some recently reported Cu²⁺ and Al³⁺ sensors (Table 1).

Please insert **Table 1**

The binding stoichiometry of the **7a**-Cu²⁺ complex was determined using the continuous variations (Job's method) method (Fig. S8 a, ESI †). When the molar fraction of the sensor was 0.5, the absorbance value approached a maximum, which demonstrated the formation of a 1:1 complex between the receptor sensor and Cu²⁺. The similar trend observed for **7b**-Al³⁺ complex (Fig. S8 b, ESI †). The reaction media was investigated to obtain a suitable reaction system. The fluorescence response of **7a** (20 μM) with Cu²⁺ (5 equiv.) was studied in different solvents such as CH₃CN, MeOH, EtOH and DMF. It was observed that in CH₃CN the fluorescence intensity of **7a**-Cu²⁺ was slightly higher than the MeOH and EtOH. However, noticeable decrease in the fluorescence intensity was observed for DMF (Fig. S9, ESI †). So, CH₃CN was chosen as the solvents for the analyses. The binding of Cu²⁺ with **7a** and Al³⁺ with **7b** was further supported by ¹H NMR study in DMSO-*d*₆ (Fig. S14 and S15, ESI †). The interaction of Cu²⁺ or Al³⁺ with the probes takes place through carboxylic oxygen and nitrogen lone-pairs present in the receptor part of the molecule. Other part of the molecule is not involved in the complex formation with Cu²⁺ and Al³⁺. Upon the addition of metal to **7a** and **7b** the shift in the signals for receptor protons adjacent to carboxylic acid group was not observed. In contrast, before addition of metal ions the probes **7a** and **7b** showed signal at $\delta = 12.67 \text{ ppm}$ and $\delta = 12.17 \text{ ppm}$ respectively accounting for two acid protons. But after addition of one equivalent Cu²⁺ to

probe **7a** and Al^{3+} to the probe **7b**, the signal at $\delta = 12.67$ ppm and $\delta = 12.17$ ppm disappeared which supports the binding of Cu^{2+} and Al^{3+} to the probe **7a** and **7b** through -COOH group.

3. Experimental:

3.1. Methods and materials

All the reagents were purchased from S. D. Fine Chemical Limited (India) of commercial grade and used without further purification. All the common chemicals were of analytical grade. The solvents were purified by standard procedures. All the reactions were monitored by TLC (thin-layer chromatography) with detection by UV light. The absorption spectra of the chromophores were recorded on Perkin-Elmer spectrophotometer, Lambda 25. The emission spectra were recorded on Varian Cary Eclipse fluorescence spectrophotometer. The freshly prepared solutions in solvents of different polarities at a concentration of 1×10^{-6} mol L^{-1} solution were used in 1 cm optical path length quartz cuvette. The photophysical properties were investigated using solvatochromic and solvatofluoric behaviours of the chromophores. The excitation wavelength used for fluorescence measurements as absorption maxima of the compounds in respective solvents. The FT-IR spectra were recorded on a Perkin-Elmer Spectrum 100 FT-IR Spectrometer. ^1H NMR spectra were recorded on Varian 500 MHz instrument using TMS as an internal standard. Mass spectra were recorded on Finnigan mass spectrometer.

3.2. Preparation of salt solution

The commercially available salts such as $\text{ZnCl}_2 \cdot 6\text{H}_2\text{O}$, HgCl_2 , CdCl_2 , $\text{FeCl}_2 \cdot 4\text{H}_2\text{O}$, $\text{BaCl}_2 \cdot 2\text{H}_2\text{O}$, $\text{MnCl}_2 \cdot 4\text{H}_2\text{O}$, $\text{NiCl}_2 \cdot 6\text{H}_2\text{O}$, $\text{MgCl}_2 \cdot 6\text{H}_2\text{O}$, $\text{CoCl}_2 \cdot 6\text{H}_2\text{O}$, $\text{CuCl}_2 \cdot 2\text{H}_2\text{O}$, CuCl , NaCl , KCl , AgNO_3 and

Al(NO₃)₃·9H₂O were used to prepare the stock solution of metal ions in double distilled deionise water at room temperature.

Quantum yields determinations

The relative quantum yields of synthesized compounds in different solvents were calculated by using equation 1. The refractive indices of the solvents have been taken from literature⁵⁵. The quantum yields of the sensors **7a-b** were evaluated in free as well as metal bound form in acetonitrile at room temperature by using quinine sulfate in 0.1 N H₂SO₄ (Φ_f = 0.51) as a standard^{55,56}.

$$\phi_x = \Phi_{st} \times \frac{Grad_x}{Grad_{st}} \times \frac{\eta_x^2}{\eta_{st}^2} \dots\dots\dots (1)$$

Where:

Φ_x = Quantum yield of compound, Φ_{st} = Quantum yield of standard sample

Grad_x = Gradient of compound, Grad_{st} = Gradient of standard sample

η_x = Refractive index of solvent used for synthesized compound

η_{st} = Refractive index of solvent used for standard sample

3.3.Synthesis

3.3.1. Synthesis of intermediate 4

Phosphorous oxychloride (POCl₃) (2.75 ml, 0.03 mol) was slowly added to dimethyl formamide (DMF) (3.65 mL, 0.05 mol) at 5–10 °C under constant stirring. To this cooled reagent *N*-substituted

amino benzene (0.01 mmol) was added by dissolving it in DMF (6 mL) under constant stirring and the resulting mixture was heated at 75 °C for 4 h. The reaction mixture was cooled to room temperature and then poured into ice cold water (60 mL). The reaction mass was neutralized with sodium carbonate and extracted by ethyl acetate. The organic layer was dried by sodium sulphate and evaporated on rotary evaporator offered brown colored liquid which was used for the further reaction. Yield: 85 %. FT-IR (cm⁻¹): 1730 (ester), 1705 (aldehyde), 1650, 1600 (-C=C-, aromatic). ¹H NMR (500 MHz, CDCl₃, ppm, Me₄Si): δ = 2.62 (t, 4H, -CH₂), 3.68 (s, 6H, -CH₃), 3.75 (t, 4H, -CH₂), 6.71 (d, *J* = 9 Hz, 2H), 7.72 (d, *J* = 9 Hz, 2H), 9.72 (s, 1H). ¹³C NMR (125.6 MHz, CDCl₃, ppm, Me₄Si): 32.0, 46.7, 51.9, 111.2, 126.0, 132.2, 151.3, 171.9, 190.2.

3.3.2. Synthesis of Intermediate 5a-b

Dimedone (2.0 mmol) and substituted aromatic aldehydes (1.0 mmol) were stirred in ethylene glycol at 80 °C for 6 h. The progress of the reaction was monitored by TLC. After completion of reaction, the reaction mixture was poured in water the obtained solid was filtered and dried. The crude product was recrystallized from 95 % ethanol.

5a: Yield = 95%, Melting point: 190 °C. FT-IR (cm⁻¹): 2955 (-CH), 1770, 1740 (ester), 1665 (ketone), 1530 (-C=C-, aromatic). ¹H NMR (500 MHz, CDCl₃, ppm, Me₄Si): δ = 1.09 (s, 6H, -CH₃), 1.21 (s, 6H, -CH₃), 2.35 (m, 10 H), 3.79 (s, 6H), 4.11 (s, 4H), 5.43 (s, 1H), 6.52 (d, *J* = 9 Hz, 2H), 6.92 (d, *J* = 9 Hz, 2H). ¹³C NMR (125.6 MHz, CDCl₃, ppm, Me₄Si): 27.3, 29.7, 31.3, 46.4, 47.1, 52.1, 53.3, 112.4, 115.7, 127.8, 145.8, 171.5, 190.2. Mass: *m/z* 527.4 [M]⁺.

5b: Yield = 93%, Melting point: 195 °C. FT-IR (cm⁻¹): 2954 (-CH), 1766, 1741 (ester), 1662 (ketone), 1519 (-C=C-, aromatic). ¹H NMR (500 MHz, CDCl₃, ppm, Me₄Si): δ = 1.09 (s, 6H, -CH₃), 1.22 (s, 6H, -CH₃), 2.38 (broad, 10 H), 2.57 (t, 4H), 3.61 (t, 4H), 3.66 (s, 6H, -CH₃), 5.44 (s, 1H),

6.61 (d, $J = 9$ Hz, 2H), 6.93 (d, $J = 9$ Hz, 2H). ^{13}C NMR (125.6 MHz, CDCl_3 , ppm, Me_4Si): 27.1, 29.7, 31.3, 31.8, 32.3, 46.4, 46.9, 51.7, 112.5, 115.8, 127.9, 144.7, 172.5, 190.3. Mass: m/z 556.9 $[\text{M}+\text{H}]^+$.

3.3.3. Synthesis of Intermediate 6a-b

The tetraketone intermediates **5a-b** (1.0 mmol) were taken in aq. ethanol and ammonium acetate (3.0 mmol) was added and the reaction mixture heated for 6 h. The progress of the reaction was monitored by TLC. Ethanol was evaporated and diluted by water. The obtained solid was filtered and dried. The crude product was recrystallized from 95% ethanol.

6a: Yield = 91%, Melting point: 210 $^{\circ}\text{C}$. FT-IR (cm^{-1}): 2960 (-CH), 1727 (ester), 1661 (ketone), 1608, 1514 (-C=C-, aromatic). ^1H NMR (500 MHz, $\text{DMSO-}d_6$, ppm, Me_4Si): $\delta = 0.87$ (s, 6H, $-\text{CH}_3$), 0.98 (s, 6H, $-\text{CH}_3$), 1.98 - 2.12 (2d, $J = 16$ Hz, 4H $-\text{CH}_2$), 2.35 (s, 4H), 3.79 (s, 6H), 3.98 (s, 4H), 4.77 (s, 1H), 6.26 (d, $J = 9$ Hz, 2H), 6.91 (d, $J = 9$ Hz, 2H). ^{13}C NMR (125.6 MHz, $\text{DMSO-}d_6$, ppm, Me_4Si): 27.3, 29.4, 32.0, 32.6, 46.4, 50.8, 53.4, 111.1, 112.3, 128.6, 136.5, 145.9, 149.3, 173.1, 194.8. Mass: m/z 479.51 $[\text{M}-\text{H}]^+$.

6b: Yield = 92%, Melting point: 221 $^{\circ}\text{C}$. FT-IR (cm^{-1}): 2963 (-CH), 1729 (ester), 1666 (ketone), 1618, 1519 (-C=C-, aromatic). ^1H NMR (500 MHz, $\text{DMSO-}d_6$, ppm, Me_4Si): $\delta = 0.99$ (s, 6H, $-\text{CH}_3$), 1.07 (s, 6H, $-\text{CH}_3$), 1.98 - 2.12 (2d, $J = 16$ Hz, 4H, $-\text{CH}_2$), 2.32 (m, 4H), 2.52 (t, 4H), 3.55 (t, 4H), 3.64 (s, 6H), 4.97 (s, 1H), 6.62 (d, $J = 9$ Hz, 2H), 7.16 (d, $J = 9$ Hz, 2H). ^{13}C NMR (125.6 MHz, $\text{DMSO-}d_6$, ppm, Me_4Si): 27.4, 29.3, 32.4, 31.7, 41.3, 47.0, 50.8, 51.6, 112.3, 114.1, 129.0, 135.7, 144.9, 146.9, 172.7, 195.3. Mass: m/z 537.5 $[\text{M}+\text{H}]^+$.

Synthesis of sensors 7a-b

The ester intermediates **6a-b** (1.0 mmol) were taken in aq. ethanol and 10% sodium hydroxide (3.0 mmol) was added and the reaction mixture refluxed for 2 h. The progress of the reaction was monitored by TLC. Ethanol was evaporated and water (10 ml) was added in the residue. The resultant reaction mass acidified by dil. HCl to pH 6. The obtained solid was filtered, dried and recrystallized using by 95% ethanol.

7a: Yield = 91%, Melting point: 227 °C. FT-IR (cm⁻¹): 2963 (-CH), 1729 (acid), 1666 (ketone), 1618, 1519 (-C=C-, aromatic). ¹H NMR (500 MHz, DMSO-*d*₆, ppm, Me₄Si): δ = 0.87 (s, 6H, -CH₃), 0.98 (s, 6H, -CH₃), 1.98 - 2.12 (2d, *J* = 16 Hz, 4H -CH₂), 2.35 (s, 4H), 3.98 (s, 4H), 4.67 (s, 1H), 6.26 (d, *J* = 9 Hz, 2H), 6.91 (d, *J* = 9 Hz, 2H), 9.15 (s, 1H, NH), 12.67 (s, 2H). ¹³C NMR (125.6 MHz, DMSO-*d*₆, ppm, Me₄Si): 27.3, 29.4, 32.0, 32.6, 50.8, 53.4, 111.1, 112.3, 128.6, 136.5, 145.9, 149.3, 173.1, 194.9. HRMS *m/z* [M+Na]⁺ Calcd for C₂₇H₃₂N₂O₆Na: 503.2158. Found: 503.2159. Mass: *m/z* 503.59 [M+Na]⁺.

7b: Yield = 92%, Melting Point: 221 °C. FT-IR (cm⁻¹): 2963 (-CH), 1732 (acid), 1636 (ketone), 1603, 1519 (-C=C-, aromatic). ¹H NMR (500 MHz, DMSO-*d*₆, ppm, Me₄Si): δ = 0.88 (s, 6H, -CH₃), 0.98 (s, 6H, -CH₃), 1.98 - 2.12 (2d, *J* = 16 Hz, 4H, -CH₂), 2.32 (s, 4H), 2.48 (t, 4H), 3.44 (t, 4H), 4.67 (s, 1H), 6.45 (d, *J* = 9 Hz, 2H), 6.93 (d, *J* = 9 Hz, 2H), 9.15 (s, 1H, NH), 12.17 (s, 2H). ¹³C NMR (125.6 MHz, DMSO-*d*₆, ppm, Me₄Si): 27.3, 29.4, 31.8, 32.5, 32.6, 46.7, 50.8, 111.8, 112.3, 128.8, 135.8, 145.1, 149.3, 173.7, 194.8. HRMS *m/z* [M+Na]⁺ Calcd for C₂₉H₃₆N₂O₆Na: 531.2471. Found: 531.2474. Mass: *m/z* 531.62 [M+Na]⁺.

4. Conclusion

In summary, we have demonstrated that the two chemosensors **7a-b** showed ideal photoinduced electron transfer behavior for the detection of Cu²⁺ and Al³⁺ respectively. The absorption spectra do

not changes significantly upon binding with various metal ion. In contrast, the emission spectra change dramatically after addition of Cu^{2+} to probe **7a** and Al^{3+} to probe **7b** even in presence of other metal ions. Upon the addition of Cu^{2+} to the probe **7a** in CH_3CN , 10 fold enhancement in the fluorescence intensity was observed. However, probe **7b** showed 15 fold enhancement in the fluorescence intensity with Al^{3+} in CH_3CN . The binding of Cu^{2+} and Al^{3+} to the sensors resulted in maximum fluorescence enhancement in the pH range of 7.0 - 9.0. The limit of detection (LOD) came out to be 2.8×10^{-7} M for **7a**- Cu^{2+} and 5.8×10^{-7} M for **7b**- Al^{3+} complex in CH_3CN which makes **7a** and **7b** suitable candidate for the development of a potential probe for biological applications.

5. Acknowledgements

Santosh Chemate is thankful for JRF and SRF fellowship from the Principal Scientific Adviser (PSA), Government of India.

6. References

- 1 V. M. Yashchuk, S. M. Yarmoluk, V. Y. Kudrya, M. Y. Losytskyy, V. P. Tokar, V. M. Kravchenko, V. B. Kovalska, a. O. Balanda and D. V. Kryvorotenko, *Adv. Opt. Technol.*, 2008, **2008**, 1–11.
- 2 S. Mizukami, T. Nagano, Y. Urano, A. Odani and K. Kikuchi, *J. Am. Chem. Soc.*, 2002, **124**, 3920–5.
- 3 M. Wang, F. Yan, Y. Zou, L. Chen, N. Yang and X. Zhou, *Sensors Actuators B. Chem.*, 2014, **192**, 512–521.
- 4 Z. Guo, G. H. Kim, I. Shin and J. Yoon, *Biomaterials*, 2012, **33**, 7818–27.
- 5 H. Li, J. Fan and X. Peng, *Chem. Soc. Rev.*, 2013, **42**, 7943–62.
- 6 L. Zhu, Z. Yuan, J. T. Simmons and K. Sreenath, *RSC Adv.*, 2014, **4**, 20398–20440.
- 7 M. Shellaiah, Y. H. Wu and H. C. Lin, *Analyst*, 2013, **138**, 2931–42.
- 8 X. M. Xie and T. G. Smart, *Nature*, 1991, **349**, 521–4.
- 9 Z. Xu, G. H. Kim, S. J. Han, M. J. Jou, C. Lee, I. Shin and J. Yoon, *Tetrahedron*, 2009, **65**, 2307–2312.
- 10 T. Budde, A. Minta, J. White and A. Kay, *Neuroscience*, 1997, **79**, 347–358.

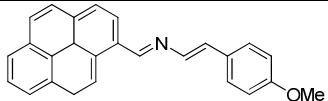
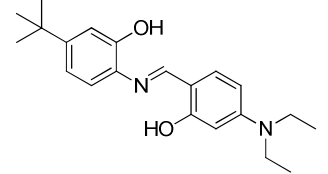
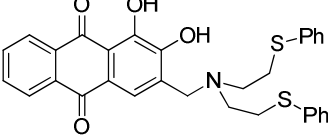
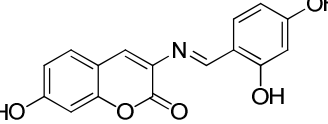
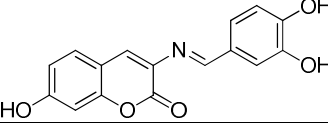
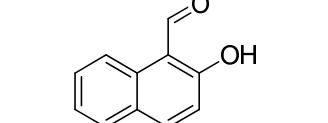
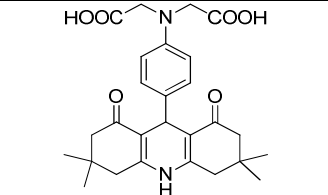
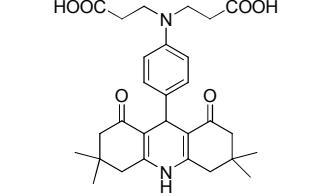
- 11 S. W. Suh, K. B. Jensen, M. S. Jensen, D. S. Silva, P. J. Kesslak, G. Danscher and C. J. Frederickson, *Brain Res.*, 2000, **852**, 274–278.
- 12 D. Strausak, J. F. Mercer, H. H. Dieter, W. Stremmel and G. Multhaup, *Brain Res. Bull.*, 2001, **55**, 175–185.
- 13 I. Scheiber, R. Dringen and J. F. B. Mercer, *Met. Ions Life Sci.*, 2013, **13**, 359–87.
- 14 D. M. Williams, *Semin. Hematol.*, 1983, **20**, 118–28.
- 15 J. Ren and H. Tian, *Sensors*, 2007, **7**, 3166–3178.
- 16 J. E. Ross, *Fd Chem.Toxic.vol .26*, 1988, **109**, 20.
- 17 C. Exley, L. M. Charles, L. Barr, C. Martin, A. Polwart and P. D. Darbre, *J. Inorg. Biochem.*, 2007, **101**, 1344–6.
- 18 E. B. Lindblad, B. Biosector and D. Frederikssund, *Immunol. Cell Biol.*, 2004, **82**, 497–505.
- 19 A. Lione, *Gen. Pharmacol. Vasc. Syst.*, 1985, **16**, 223–228.
- 20 L. D. A. L. Bo, G. Broccali and G. B. Porrol, *Antimicrob. Agent Chemother.*, 1993, **37**.
- 21 B. S. M. Beekman, *J. Am. Pharm. Assoc.*, 1959, **49**, 191–200.
- 22 S. Jain, S. Khare, A. Sharma, V. Budhiraja and R. Rastogi, *People's J. Sci. Res.*, 2009, **2**, 1–4.
- 23 N. Embi, A. Suhaimi, R. Mohamed and G. Ismail, *Microbiol. Immunol.*, 1992, **36**, 899–904.
- 24 R. A. Yokel, in *NeuroToxicology*, 2000, vol. 21, pp. 813–828.
- 25 T. P. Flaten, *Brain Res. Bull.*, 2001, **55**, 187–196.
- 26 M. Baral, S. K. Sahoo and B. K. Kanungo, *J. Inorg. Biochem.*, 2008, **102**, 1581–8.
- 27 V. K. Gupta, A. K. Jain and G. Maheshwari, *Talanta*, 2007, **72**, 1469–73.
- 28 N. E. W. Alstad, B. M. Kjelsberg, L. A. Vøllestad, E. Lydersen and A. B. S. Poléo, *Environ. Pollut.*, 2005, **133**, 333–42.
- 29 E. Delhaize and P. R. Ryan, *Plant Physiol.*, 1995, **107**, 315–321.
- 30 J. Barceló and C. Poschenrieder, *Environ. Exp. Bot.*, 2002, **48**, 75–92.
- 31 M. Porento, V. Sutinen, T. Julku and R. Oikari, *Appl. Spectrosc.*, 2011, **65**, 678–83.
- 32 J. Jebali, M. Banni, H. Gerbej, H. Boussetta, J. López-Barea and J. Alhama, *Mar. Environ. Res.*, 2008, **65**, 358–63.

- 33 X. Zhu, H. Yu, H. Jia, Q. wu, J. Liu and X. Li, *Anal. Methods*, 2013, **5**, 4460.
- 34 F. Hegedüs, P. Wobrauschek, C. Strelí, P. Winkler, R. Rieder, W. Ladisich, M. Victoria, R. W. Ryon and W. F. Sommer, *X-Ray Spectrom.*, 1995, **24**, 253–254.
- 35 J. Otero-Romaní, A. Moreda-Piñeiro, P. Bermejo-Barrera and A. Martín-Esteban, *Talanta*, 2009, **79**, 723–9.
- 36 G. Liu, Q. T. Nguyen, E. Chow, T. Böcking, D. B. Hibbert and J. J. Gooding, *Electroanalysis*, 2006, **18**, 1141–1151.
- 37 T. Q. Duong and J. S. Kim, *Chem. Rev.*, 2010, **110**, 6280–301.
- 38 C. Kar, M. D. Adhikari, A. Ramesh and G. Das, *Inorg. Chem.*, 2013, **52**, 743–52.
- 39 Z. Xu, Y. Xiao, X. Qian, J. Cui and D. Cui, *Org. Lett.*, 2005, **7**, 1053–1056.
- 40 G. He, X. Zhao, X. Zhang, H. Fan and S. Wu, *New J. Chem.*, 2010, **34**, 1055–1058.
- 41 S. Sarkar, S. Roy, A. Sikdar, R. N. Saha and S. S. Panja, *Analyst*, 2013, **138**, 7119–26.
- 42 C. Kar, M. D. Adhikari, B. K. Datta, A. Ramesh and G. Das, *Sensors Actuators B Chem.*, 2013, **188**, 1132–1140.
- 43 K. Soroka, R. S. Vithanage, D. a. Phillips, B. Walker and P. K. Dasgupta, *Anal. Chem.*, 1987, **59**, 629–636.
- 44 S. C. Warren-Smith, S. Heng, H. Ebendorff-Heidepriem, A. D. Abell and T. M. Monro, *Langmuir*, 2011, **27**, 5680–5.
- 45 D. Maity and T. Govindaraju, *Inorg. Chem.*, 2010, **49**, 7229–31.
- 46 X. Li, J. Chen and E. Wang, *Chinese J. Chem.*, 2014, **32**, 429–433.
- 47 S. H. Kim, H. S. Choi, J. Kim, S. J. Lee, T. Quang and J. S. Kim, *Org. Lett.*, 2010, **12**, 987–990.
- 48 S. Kim, J. Y. Noh, K. Y. Kim, J. H. Kim, H. K. Kang, S. Nam, S. H. Kim, S. Park, C. Kim and J. Kim, *Inorg. Chem.*, 2012, **51**, 3597–602.
- 49 W. Lin, L. Yuan and J. Feng, *European J. Org. Chem.*, 2008, **2008**, 3821–3825.
- 50 Z. Xu, J. Yoon and D. R. Spring, *Chem. Soc. Rev.*, 2010, **39**, 1996–2006.
- 51 A. P. de Silva, T. S. Moody and G. D. Wright, *Analyst*, 2009, **134**, 2385–93.
- 52 A. P. de Silva, H. Q. N. Gunaratne, T. Gunnlaugsson, A. J. M. Huxley, C. P. McCoy, J. T. Rademacher and T. E. Rice, *Chem. Rev.*, 1997, **97**, 1515–1566.

- 53 A. P. de Silva, H. Q. N. Gunaratne, T. Gunnlaugsson and M. Nieuwenhuizen, *Chem. Commun.*, 1996, 1967.
- 54 W. Zhu, X. Huang, Z. Guo, X. Wu, H. Yu and H. Tian, *Chem. Commun. (Camb.)*, 2012, **48**, 1784–6.
- 55 M. K. Saroj, N. Sharma and R. C. Rastogi, *J. Fluoresc.*, 2011, **21**, 2213–27.
- 56 T. Royal, *J. Photochem.*, 1983, **23**, 193–217.
- 57 F. Zapata, A. Caballero, A. Espinosa and P. Molina, *Org. Lett.*, 2006, **8**, 57–60.
- 58 U. N. Yadav, P. Pant, S. K. Sahoo and G. S. Shankarling, *RSC Adv.*, 2014, **4**, 42647–42653.
- 59 Y. Lu, S. Huang, Y. Liu, S. He, L. Zhao and X. Zeng, *Org. Lett.*, 2011, **13**, 5274–7.
- 60 O. García-Beltrán, B. K. Cassels, C. Pérez, N. Mena, M. T. Núñez, N. P. Martínez, P. Pavez and M. E. Aliaga, *Sensors (Basel)*, 2014, **14**, 1358–71.
- 61 Y. W. Liu, C. H. Chen and A. T. Wu, *Analyst*, 2012, **137**, 5201–3.

.....Table.....

Table 1. Performance comparison of various chemosensors reported for Cu²⁺ and Al³⁺ detection.

Sr. No.	Receptor	Metal Ion	Association Constant (K _a)(M ⁻¹)	Limit of Detection (M)	Reference
1		Cu ²⁺	8.55 x 10 ⁵	2.55 x 10 ⁻⁶	[57]
2		Cu ²⁺	1.5 x 10 ⁴	1.15 x 10 ⁻⁶	[58]
3		Al ³⁺	8.84 x 10 ³	5.0 x 10 ⁻⁷	[59]
4		Cu ²⁺	NA	1.0 x 10 ⁻⁴	[60]
5		Cu ²⁺	NA	1.0 x 10 ⁻⁴	[60]
6		Al ³⁺	8.32 x 10 ⁶	3.28 x 10 ⁻⁶	[61]
7		Cu ²⁺	4.0 x 10 ⁴	2.8 x 10 ⁻⁷	This work
8		Al ³⁺	1.7 x 10 ⁴	5.8 x 10 ⁻⁷	This work

.....**Figures all**.....

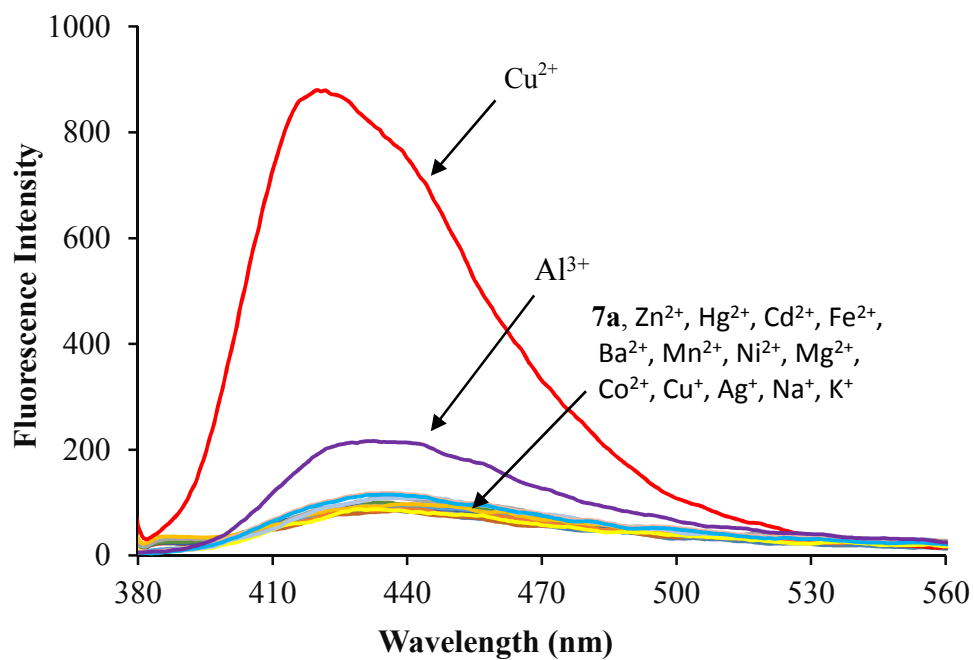


Fig. 1 Fluorescence emission spectra of **7a** (20 μM) upon addition of various metal ions (5 equiv.) in CH₃CN. λ_{exc} = 365 nm (Slit widths: 5 nm/5 nm).

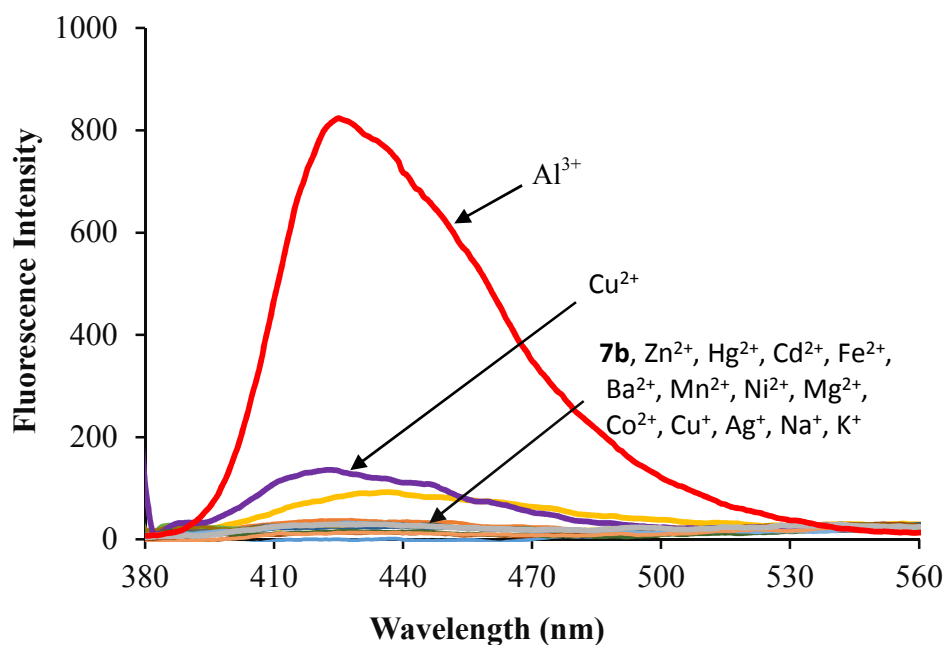


Fig. 2 Fluorescent emission spectra of **7b** (20 μM) upon addition of various metal ions (5 equiv.) in CH_3CN . $\lambda_{\text{ex}} = 365$ nm (Slit widths: 5 nm/5 nm).

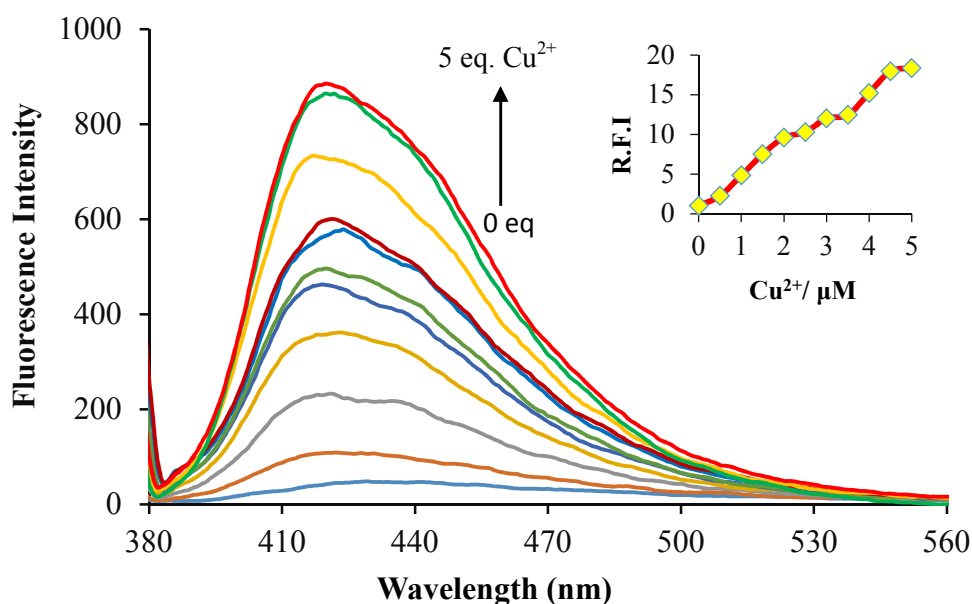


Fig. 3 Changes in the fluorescence emission spectra of probe **7a** (10 μM) in CH_3CN upon titration with 0 to 5.0 equiv. of Cu^{2+} . Inset: The relative fluorescence intensity (R.F.I) at 420 nm as a function of Cu^{2+} ion concentration. $\lambda_{\text{ex}} = 365$ nm (Slit widths: 5 nm/5 nm).

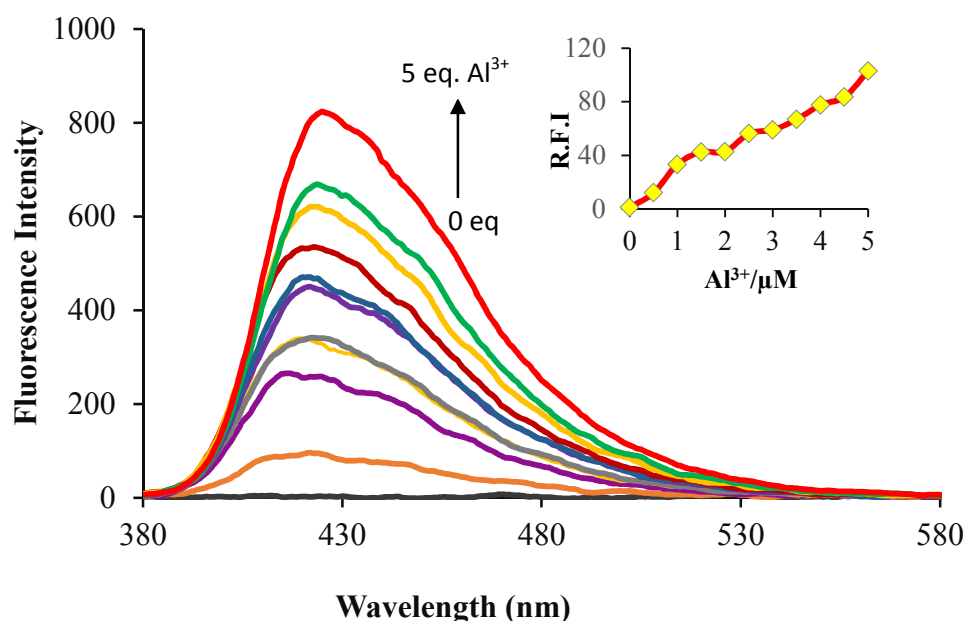


Fig. 4 Changes in the fluorescence emission spectra of probe **7b** (10 μM) in CH_3CN upon titration with 0 to 5.0 equiv. of Al^{3+} . Inset: The relative fluorescence intensity (R.F.I) at 427 nm as a function of Al^{3+} ion concentration. $\lambda_{\text{exc}} = 365$ nm (Slit widths: 5 nm/5 nm).

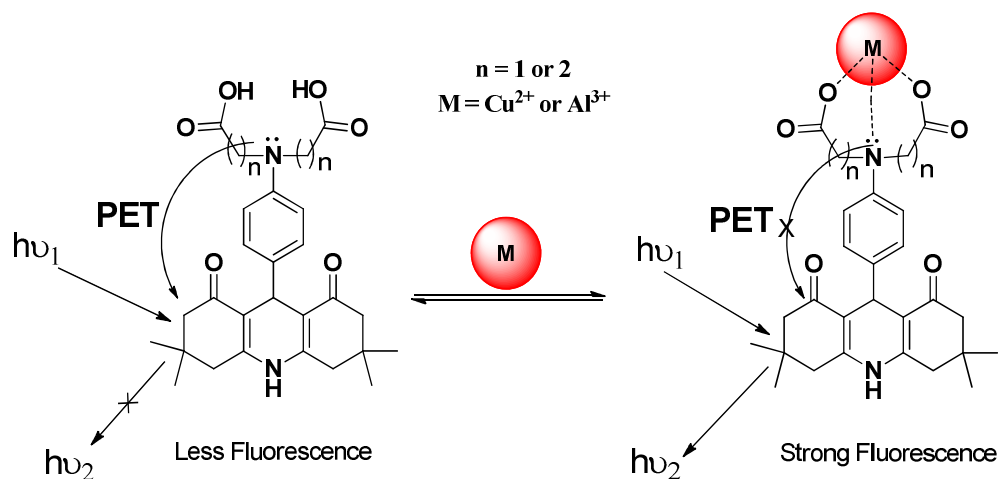


Fig. 5 Proposed binding mechanism of Cu^{2+} and Al^{3+} with sensors **7a** and **7b**.

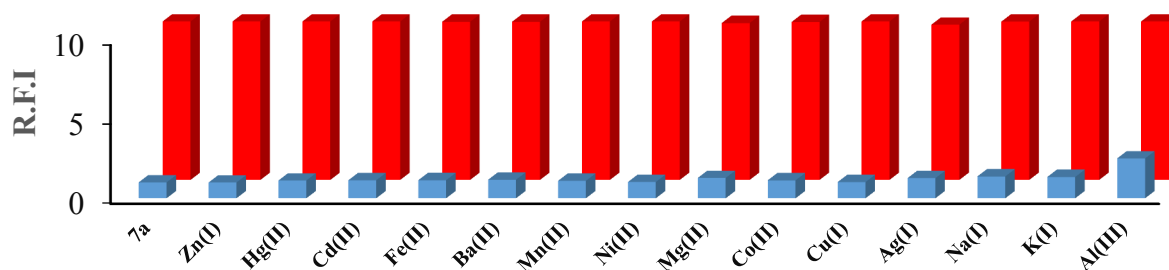


Fig. 6 Relative fluorescent intensity (R.F.I.) of probe **7a** (10.0 μM) in presence of 2.0 equiv. other metal ions (blue bars) in CH_3CN . The red bars represent the change of the emission that occurs upon the subsequent addition of 2.0 equiv. of Cu^{2+} to above solution (25 $^\circ\text{C}$), $\lambda_{\text{ex}} = 365 \text{ nm}$ (Slit widths: 5 nm/5 nm).

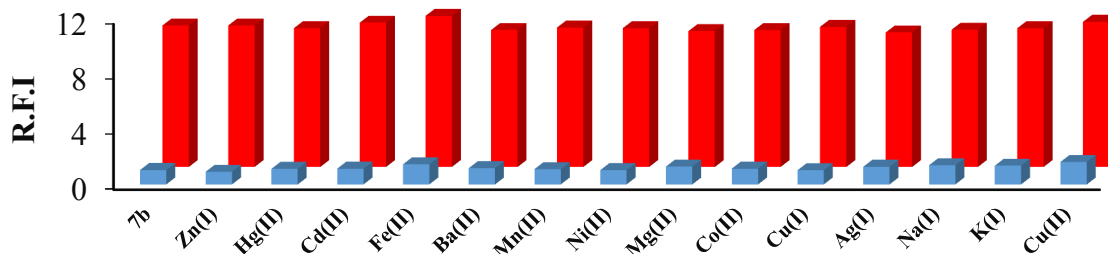


Fig. 7 Relative fluorescent intensity (R.F.I.) of probe **7b** (10.0 μM) in presence of 2.0 equiv. other metal ions (blue bars) in CH_3CN . The red bars represent the change of the emission that occurs upon the subsequent addition of 2.0 equiv. of Al^{3+} to above solution (25 $^\circ\text{C}$), $\lambda_{\text{ex}} = 365 \text{ nm}$ (Slit widths: 5 nm/5 nm).